JOURNAL OF GEOPHYSICAL RESEARCH, VOL. 113, D05206, doi:10.1029/2007JD008636, 2008

Click Here for Full Article

Aerosol properties over the SAFARI-2000 area retrieved from ATSR-2

C. Robles-Gonzalez[1] and G. de Leeuw[2,3]

Received 8 March 2007; revised 22 October 2007; accepted 10 December 2007; published 11 March 2008.

[1] The aerosol optical depth (AOD) at three wavelengths has been retrieved from the radiance measured at the top of the atmosphere (TOA) by the ATSR-2 (Along Track Scanning Radiometer) during the SAFARI-2000 (Southern African Regional Science Initiative) dry season field campaign from 1 August to 30 September 2000. Two aerosol types were implemented in the ATSR-2 retrieval algorithm: a highly absorbing aerosol that is mainly due to biomass burning and a less absorbing mixture of biomass burning, anthropogenic and biogenic aerosols. The mixing ratio of these two aerosol types was determined by comparison of the two modeled aerosol types with the ATSR-2 measured signal. The accuracy of the AOD values determined from the ATSR-2 data is 0.08 ± 0.06 for August and 0.14 ± 0.13 for September, as determined from comparison with various AERONET Sun photometers located in the area. In August 2000, the highly absorbing aerosol was the major aerosol component retrieved over the North-Western part of the SAFARI-2000 area. AOD values of up to 0.8 and Ångström coefficients of up to 2.1 were observed. Further to the South, the less absorbing type dominated with AOD values of up to 0.3 over the central SAFARI-2000 area. During September the meteorological situation changed and the high absorbing aerosols were observed further South, due to advective transport of aerosol over a wider area. AOD values were up to 1 with Ångström coefficients similar to those in August. Low absorbing aerosols were observed over a relatively small area. Over the Namibian and Kalahari deserts dust emissions caused high AOD values of up to 0.75 during both months.

Citation: Robles-Gonzalez, C., and G. de Leeuw (2008), Aerosol properties over the SAFARI-2000 area retrieved from ATSR-2, *J. Geophys. Res.*, *113*, D05206, doi:10.1029/2007JD008636.

1. Introduction

[2] The reflectance and absorbance of solar radiation by aerosols affect the Earth's radiation balance (the direct aerosol effect). Reflection increases the atmospheric albedo, causing negative radiative forcing and therefore cooling of the atmosphere. In the *IPCC* [2007] assessment report the total direct aerosol radiative forcing as derived from models and observations is estimated to be -0.5 [±0.4] W m^{-2}, with a medium-low level of scientific understanding. Improved satellite measurements have contributed to the increase of the level of scientific understanding since the third IPCC assessment report in 2001. The continued improvement of aerosol retrieval from satellite based instruments, to provide consistent information with a known level of accuracy, is important to further our understanding of climate and climate change. This paper aims to contribute with the development of algorithms for the ATSR-2 (Along Track Scanning Radiometer) for the retrieval of aerosol properties over land. The importance of ATSR is the potential of a long time series starting with ATSR launched in 1995 on ERS-1, continued with AATSR on ENVISAT, which provides a 12-year data series (and continuing) and plans for an ATSR-like instrument (SLST) on Sentinel-3.

[3] Globally the net aerosol radiative forcing is negative but on local scales absorbing aerosols can cause net positive radiative forcing resulting in warming of the atmospheric layer. Two of the major sources of absorbing aerosols are biomass burning (BB) and fossil fuel (FF) burning [*IPCC*, 2001]. The positive or negative radiative forcing effect of these two aerosol types strongly depends on their black carbon (BC) content, which in turn depends on the combustion phase in which the aerosol is created [*Ward et al.*, 1992, 1996].

[4] BB emissions are strongly seasonal [*Iacobellis et al.*, 1999]. Because they are formed near the surface and are mainly located in the boundary layer they have a relatively short atmospheric residence time and hence their influence on climate is regional and seasonal. In order to evaluate and better understand the effects of BB and FF aerosols, campaigns such as SAFARI-2000 have been carried out [*Swap et al.*, 2002]. SAFARI-2000 was conducted over Southern Africa during the dry season in August and September 2000.

[5] The aim of the work described in this paper is to develop an algorithm to retrieve aerosol properties over an area governed by BB aerosol. The SAFARI-2000 area was

[1]National Spanish Institute for Aerospace Technology (INTA), Madrid, Spain.
[2]Finnish Meteorological Institute, R&D, Climate Change Unit, Modelling and Observation of Atmosphere, Helsinki, Finland.
[3]Department of Physical Sciences, University of Helsinki, Helsinki, Finland.

Copyright 2008 by the American Geophysical Union.
0148-0227/08/2007JD008636$09.00

chosen because of the availability of in situ data that can be used either for the algorithm development or for comparison with the retrieval results. To reach this goal, two aerosol types with different properties, mainly different imaginary part of the refractive index, have been implemented in our aerosol retrieval algorithms for ATSR-2 following the work described by *Robles-Gonzalez et al.* [2006]. The retrieval of absorbing aerosol types renders problems because satellite sensors measure reflectance which due to absorption is reduced in the measured signal at the TOA. Hence the problem is to determine whether the signal at the TOA is due to scattering aerosols or from a combination of scattering and absorption. The wavelength dependence is an essential tool since these situations have a different spectral behavior. Furthermore, a priori information on the expected aerosol types is used from measurements, models and climatologies [*Robles González et al.*, 2006]. In this case, aerosol properties from the SAFARI-2000 measurements were used, i.e., column integrated effective aerosol properties from *Dubovik et al.* [2002] and the AERONET web site [http://aeronet.gsfc.nasa.gov]. The challenge was to determine the optimum mixing ratio of the two aerosol types mentioned above, i.e., the mixing ratio of the aerosol types was determined by the algorithm by application of the least squares error function at different wavelengths, this fit providing similar results as ground-based measurements throughout the area. For this study we used radiances measured with the Along Track Scanning Radiometer (ATSR-2) on board the ERS-2 (European Remote Sensing) satellite. AERONET Sun photometers [*Holben et al.*, 1998] in the SAFARI-2000 area were used for comparison of the retrieved AOD with independent ground-based data. The ATSR-2 dual view (DV) algorithm [*Veefkind et al.*, 1998] provided not only the AOD and Ångström coefficient, but also the relative contribution of two aerosol types to the total AOD over the SAFARI-2000 region. The use of ATSR-2 data for retrieval over the Atlantic Ocean west of the SAFARI area was demonstrated by *Schmid et al.* [2003].

2. ATSR-2 Sensor

[6] The ATSR-2 [*Stricker et al.*, 1995] on board the European Remote Sensing Satellite ERS-2 was launched in April 1995. It is a radiometer with seven wavelength bands, four of which are in the visible and near-infrared parts of the spectrum (effective wavelengths 0.555, 0.659, 0.865, and 1.6 μm). These four channels are used for the retrieval of the AOD. The three thermal infrared bands are used in this paper for cloud detection and cloud masking. In-flight calibration is done by measuring the solar irradiance during some parts of the ATSR-2 orbit. The ATSR-2 has a conical scanning mechanism providing two views of each location: first a forward view (viewing zenith angle approximately 56°) and about two minutes later a nadir view. The spatial resolution is approximately 1×1 km^2 at nadir. The swath width of the ATSR-2 is 512 km. The overpass time of ATSR-2 is around 10:30 local solar time.

3. SAFARI-2000 Campaign

[7] The SAFARI-2000 campaign was conducted over Southern Africa (Figure 1) from 1st August until 30th September 2000, i.e., during the dry season [*Swap et al.*, 2002]. The goal of this campaign was to evaluate the biogenic, pyrogenic and anthropogenic emissions and better understand the physical, chemical and radiative processes that affect the African ecosystem. During the SAFARI-2000 experiment three major aerosol sources were found [*Swap et al.*, 2002]:

[8] 1. FF burning aerosol from industrial activities that have been developed in the last years due to the improvement of the economical and political situation.

[9] 2. BB from man-made and natural fires. BB from natural fires occurs over the tropical rain forest and savanna regions located in the North-Western part of the SAFARI-2000 area. In this area the vegetation is abundant. Domestic fires are sparse over the entire area. Aerosols from FF and BB processes are in general the most absorbing aerosols due to their high BC content. *Dubovik et al.* [2002] found that BB aerosols from African savanna fires are the most absorbing of all major BB regions.

[10] 3. Natural emissions such as desert dust aerosols emitted by the wind-surface interaction and biogenic aerosols emitted by vegetation.

[11] During most of the dry season a strong anticyclonic gyre persisted over the area promoting the transport and mixing of particles. This situation changed in September with the transition from the dry to the wet season which had different airflow patterns, including two events with advection of significant amounts of BB aerosols to the South [*Eck et al.*, 2003].

4. Algorithm Description

[12] In order to retrieve the aerosol properties over the SAFARI-2000 area from ATSR-2 data, the DV algorithm developed by *Veefkind et al.* [1998] was extended with two aerosols types that are representative for the aerosol properties over the SAFARI-2000 area. Both aerosol types were selected based on data published by *Dubovik et al.* [2002] and results from the AERONET web site [http://aeronet.gsfc.nasa.gov]. The DV retrieval algorithm is based on three assumptions:

[13] 1. The top of atmosphere (TOA) reflectance due to an external mixture of two different aerosol types can be approximated as the weighted average of the reflectance of the individual aerosol types [*Wang and Gordon*, 1994]

[14] 2. The TOA reflectance is approximated as a linear function of the AOD [*Durkee et al.*, 1986].

[15] 3. The surface reflectance can be separated in a part due to the variation with the wavelength and another part due to the variation with the geometry [*Flowerdew and Haigh*, 1995]. This assumption has been recently reviewed by *North* [2002].

[16] The dual view algorithm accounts for multiple scattering and the bi-directional reflectance of the surface. The algorithm is based on minimizing the error function describing the difference between the computed TOA reflectances and those measured by ATSR-2. TOA reflectances were computed using aerosol models describing the physical and chemical properties of the aerosol expected to be present in the study area. A Mie scattering code [*De Rooij and van der Stap*, 1984] was used to compute the aerosol scattering matrix, which subsequently was used in a radia-

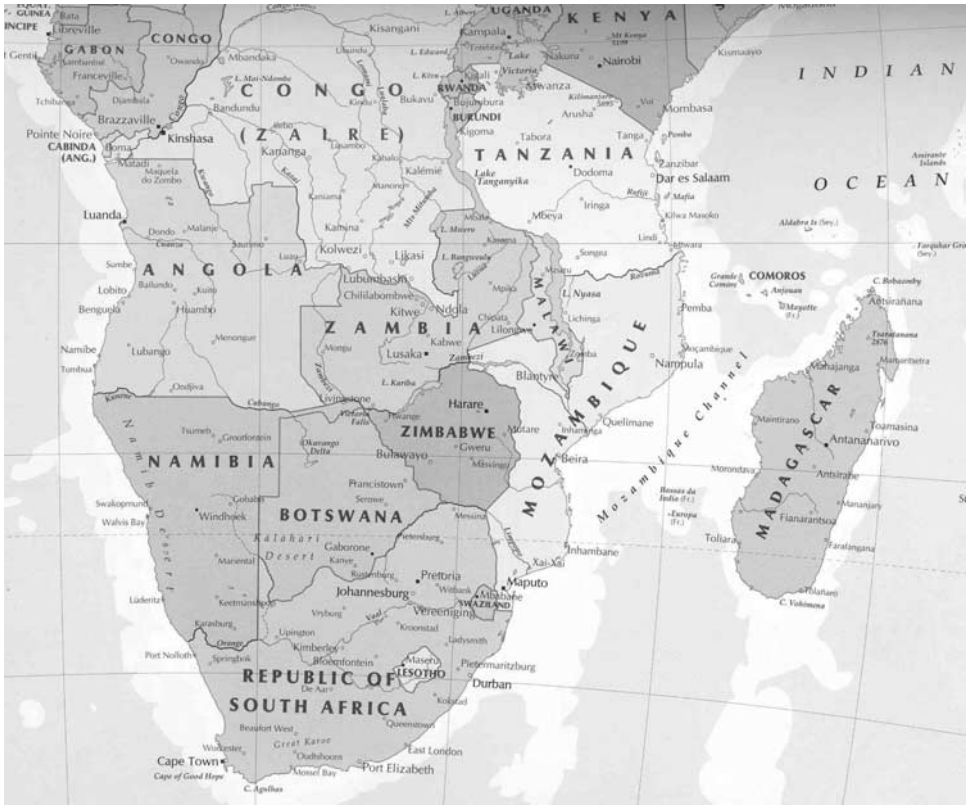

Figure 1. Political map of Africa showing the countries and the land used [The Times Atlas of the World].

tive transfer model to obtain the TOA reflectances for different sun-satellite geometries and aerosol mixtures. The radiative transfer model used was the KNMI (Royal Netherlands Meteorological Institute) Doubling and Adding model (DAK) [*Stammes*, 2001; *De Haan et al.*, 1987]. The results were used to create look up tables (LUTs) containing the calculated TOA reflection. This method was extensively described in *Robles-Gonzalez et al.* [2006].

[17] Aerosol optical properties can only be retrieved over cloud free areas. The cloud flag in the ATSR-2 data product works properly over sea but over land it is too strict and selects surfaces with high reflectance as cloudy. Therefore the ATSR-2 algorithm for cloud screening developed by *Koelemeijer et al.* [2001] has been implemented in the DV algorithm. For application to large data sets, such as SAFARI, this cloud screening algorithm has been automated as described by *Robles-Gonzalez* [2003]. Severe testing shows that the cloud screening over land is much improved with respect to the cloud product, as determined from comparison with the visual images and other cloud products.

5. Aerosol Type Selection Method

[18] Information on the aerosol refractive index retrieved from Sun photometer data at the AERONET sites can be obtained from the AERONET web site [http://aeronet.gsfc.nasa.gov]. In particular, the information available for the SAFARI area provided the basis for the further development of the ATSR-2 DV algorithm for application to the SAFARI-2000 campaign. The AERONET data show that in the southern part of the SAFARI-2000 area i.e., Bethlehem (28.33°E, 28.25°S), the mean imaginary part of the refractive index of the aerosols was lower than over the Northern areas of the campaign i.e., the sites located in Zambia, cf. Table 1. A bimodal aerosol model was constructed describing a mixture of type I and type II aerosols (cf. Table 1) in a variable mixing ratio:

$$Mmix = \frac{k_1}{(k_1 + k_2)} \tag{1}$$

where $Mmix = 1$ means that the only aerosol selected by the retrieval algorithm is aerosol type I; $Mmix = 0$ indicates that the aerosol type that best fits the measured reflectance is type II. The refractive index was selected to account for the different optical properties of the aerosols in both the northern and southern parts of the SAFARI-2000 area, as derived from the AERONET web site [http://aeronet.gsfc.nasa.gov].

[19] The algorithm searches for the aerosol mixture that best fits the spectral variation of the reflectance derived from ATSR-2 measurements by means of a least squares error function. The most appropriate aerosol mixture was determined for each ATSR-2 pixel, thus providing the spatial distribution of aerosol properties over the SAFARI area. It is noted that the input values for the model are derived from only two grid points (Bethlehem and Zambia).

[20] The aerosol type from Zambia [*Dubovik et al.*, 2002] (a highly absorbing aerosol type mainly formed by BB) is further referred as the more-absorbing type (see Table 1).

Table 1. Aerosol Properties Derived From *Dubonik et al.* [2002] and *Holben et al.* [1998][a]

	r(μm)	σ	N	k	%
Type I (fine mode)	0.080	1.490	1.51	0.0190	99.9
Type I (coarse mode)	0.705	2.075	1.51	0.0190	0.1
Type II (fine mode)	0.080	1.490	1.46	0.0148	99.5
Type II (coarse mode)	0.705	2.075	1.46	0.0148	0.5

[a]The highly absorbing aerosol type (type I) is the average of the aerosol properties measured over Zambia. The less absorbing aerosol type (type II) has the same properties as the type I except for the refractive index which is obtained from the AERONET data-base [http://aeronet.gsfc.nasa.gov]. The contribution of the coarse mode in type II is higher than in type I. Number size distribution have been used, r is the mode radius, σ is the standard deviation, n is the real part of the refractive index at 0.555 μm, and k is the imaginary part of the refractive index at 0.555 μm. The % symbol stands for the percentage contribution of the fine and coarse mode to the model.

The Bethlehem aerosol type [http://aeronet.gsfc.nasa.gov] is referred to as the less-absorbing type which is a mixture of BB, FF burning and biogenic emissions. Because of the influence of the emissions of natural aerosols on the less-absorbing aerosol type the relative contribution of coarse aerosols was assumed to be higher for this aerosol type than for the more-absorbing aerosol type.

6. Results and Discussion

6.1. Spatial Variation

[21] Composite maps of the ATSR-2 retrieved AOD at 0.555 μm, the Ångström coefficients and relative contribution of the two aerosol types over the SAFARI-2000 area are presented in Figures 2 and 3, for August and September, 2000, respectively. The data presented in Figures 2 and 3 are not an average for the whole month, rather they are a composite representative for the situation during clear sky, at the time of the ATSR-2 overpass (around 9:00 a.m. UTC), i.e., sampled every 3–4 days at a certain time. The number of available data is further reduced due to contamination by clouds. The original AOD values, with a resolution of 1 × 1 km^2, were averaged on a 10 × 10 km^2 grid, using the method described by *Robles González et al.* [2000].

[22] In Figure 2a mean AOD values of about 0.7–0.8 are observed over the North-Western part of the area, i.e., Northern Angola, and over Congo and Gabon. This area is vegetated with rain forest and savanna and it is the area where most of the fires occur [http://earthobservatory.nasa.gov; *Diner et al.*, 2001]. Hence these high AOD values were probably due to BB aerosols. AOD values of up to 0.75 were also observed over the Namibian and Kalahari deserts where natural emissions such as soil dust dominate. In the Eastern part of Tanzania and Kenya high and rather variable AOD values were observed which probably are due to emissions of dust from the dry areas. Over Mozambique relatively high AOD values of about 0.5–0.7 were observed. Mozambique and the Republic of South Africa are industrial areas, where the high AOD values could in part be due to industrial emissions. In contrast, relatively low and constant AOD values of less than 0.3 were found over most of the Central part of the SAFARI-2000 area, i.e., South of Angola and Zambia, north of Namibia and Botswana and some parts of Tanzania. This is in line with the expectation that over these areas aerosols are a mixture of BB, FF and biogenic aerosols and thus less absorbing that the aerosols from BB emissions.

[23] Ångström coefficients between 1.7 and 2.1 are observed in the North-West part of the SAFARI-2000 area, Figure 2b. These high values indicate the presence of high concentrations of fine mode particles probably from BB. In most of this figure, South of 15°S, Ångström coefficients lower than 1.2 were observed, except over some small areas where these values reached 1.4. The decrease in the Ångström coefficient values compared to those in the North indicated lower concentration of submicron particles possibly accompanied by higher concentrations of coarse particles that are usually from natural origin such as wind-blown dust. Ångström coefficients of about 1.6 in the North-East were probably due to the higher relative influence of natural emissions.

[24] In Figure 2c the mean relative contribution of the two aerosol types for August 2000 is shown. A value of one indicates that the aerosol type selected by the algorithm is the more-absorbing one while zero means that only the less-absorbing type is detected. In the North, the more-absorbing aerosol type was dominant, but the mixture gradually changed toward the South with an increasing contribution of the less-absorbing aerosol type. South of 20°S the less-absorbing aerosol type dominated during August 2000.

[25] From Figures 2a, 2b, and 2c was concluded that (a) the high AOD and Ångström coefficient values found over the North-Western part of the SAFARI-2000 region were mainly due to fine mode BB aerosols from local fires. These aerosols were highly absorbing, (b) the influence of less-absorbing aerosols increased to the South. The high AOD observed over the Namibian and Kalahari deserts was ascribed to high emissions of dust and (c) due to the anticyclone gyre that persisted over the area during August 2000, aerosol transport and mixing of BB, anthropogenic and natural aerosols occurred. This is the reason for the observation of less-absorbing aerosols South of 10°S during August 2000.

[26] In Figure 3 the composite maps of the mean AOD at 0.555 μm, Ångström coefficient and relative contribution of the two aerosol types for September 2000 are shown. The spatial distribution of the mean AOD is in good agreement with AOD results retrieved from MODIS data by *Myhre et al.* [2003] for September 2000. For this month, it was observed that high AOD values extended further to the South than in August, i.e., down to 20°S (Figure 3a). AOD values were also higher over this area, with values up to 1. The differences between August and September are due to changes in the meteorological conditions. In September, two big transport events moved high concentrations of BB aerosols from North to South [*Eck et al.*, 2003] increasing the AOD. High AOD values are observed again over the

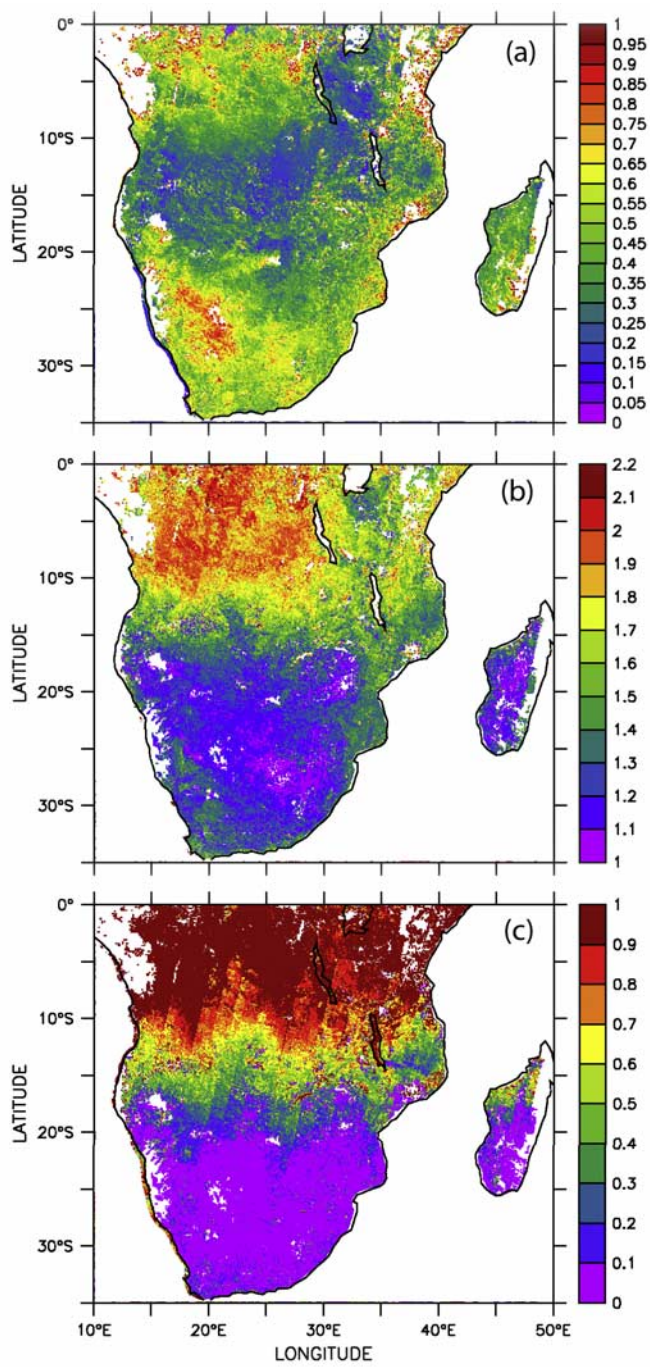

Figure 2. Composite maps of the mean (a) AOD at 0.555 μm, (b) Ångström coefficient and (c) relative contribution of a more-absorbing aerosol type (a value of one means that all the aerosol present is the more-absorbing type while zero means that only the less-absorbing type is present) retrieved over the SAFARI-2000 area during August 2000. These figures are retrieved over land using ATSR-2 data. Over white areas no data is present.

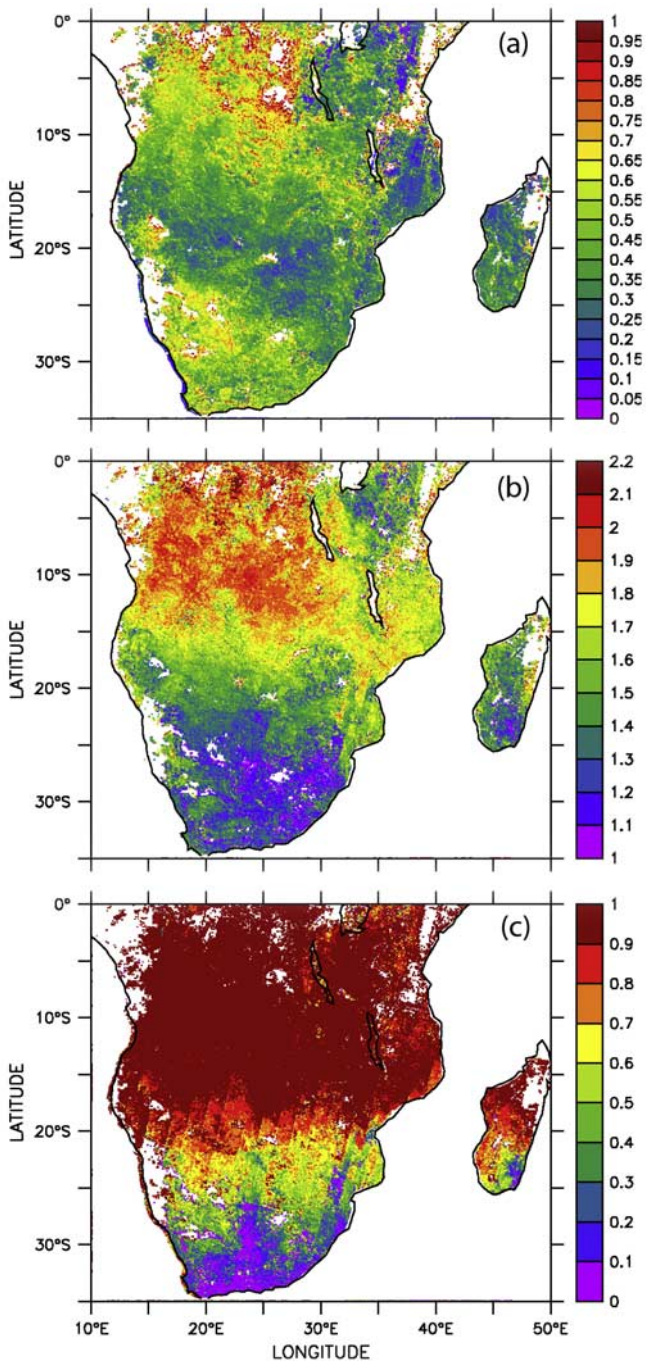

Figure 3. As Figure 2, but for September 2000.

Namibian and Kalahari Deserts. Ångström coefficients in Figure 3b show spatial trends similar to those of the AOD. High Ångström coefficients were observed as far south as 20°S. On the other hand no significant change in the values of Ångström coefficient was observed, indicating that the aerosol type over this area did not change from August to September. Ångström coefficients smaller than 1.3 were observed South of 25°S. Figure 3b confirms the presence of fine mode aerosols over most of the SAFARI-2000 area during September 2000. In Figure 3c is observed that the more-absorbing aerosol type dominated over the SAFARI-2000 area down to 20°S. The relative contribution of this aerosol type gradually decreased toward the South. The less-absorbing aerosol type dominated in a small region South of 30°S.

[27] Figures 3a–3c confirm that during September 2000 small and relatively highly absorbing aerosol types domi-

nated over the SAFARI-2000 region north of 20°S. From August to September (Figures 2 and 3) no variation in the aerosol type over the North-Western region was obvious but their concentration increased due to the change in the meteorological situation.

6.2. Comparison With AERONET Data

[28] ATSR-2 retrieved AOD values were compared with ground-based Sun photometer observations from the AERONET database [*Holben et al.*, 1998] in order to assess the accuracy of the algorithm. Examples presented in Figure 4 show both good and bad agreement. Figure 4a shows the comparison with the Sun photometer at Mwinilunga (24.43°E 11.74°S) on 17 August. This was the most Northerly AERONET station of the SAFARI-2000 area, in the burning region. The data show that the algorithm significantly underestimates the AOD and for the case with high absorbing aerosol no acceptable solution could be found. Further South, where the influence of the highly absorbing aerosol was smaller, the retrieved AOD compares much better with the Sun photometer values. This is shown in Figure 4b for Mongu (23.15°E 15.25°S) on 23 August and in Figure 4c for Solvezi (26.36°E 12.17°S) on 30 August. The mean uncertainty of the retrieved AOD compared to AERONET data and its standard deviation during August 2000 was 0.08 ± 0.06 at 0.659 μm. This uncertainty is the mean value of the AOD(ATSR-2) minus AOD(AERONET) at 0.659 μm.

[29] In Figure 4d a comparison at Skukuza (31.59°E 24.99°S) on 3 September is presented. This result is in very good agreement (within 0.02 at 0.659 μm) with the Sun photometer measurement. Note that this station is located in the Eastern part of the Republic of South Africa and thus far from the influence of the BB aerosols. From this good comparison could be concluded that the algorithm accurately retrieves the AOD of the less-absorbing aerosol types. Unfortunately no other co-located Sun photometers were found in the southern part of the SAFARI-2000 area to confirm this statement. Figures 4e and 4f show comparisons at Mongu on 8 and 24 September respectively. The comparison on 8 September included one of the two large transport events that took place during September when high aerosol concentrations were advected to the South [*Eck et al.*, 2003], causing AOD values of 0.82 at 0.670 μm measured by the Sun photometer. Retrieved AOD values were 0.39 at 0.659 μm. The comparison on 24 September after the large aerosol transport event, was much better, with the retrieved and measured AOD values within experimental uncertainty. The mean uncertainty of the retrieved AOD and its standard deviation during September 2000 was 0.14 ± 0.13.

[30] A scatterplot of AOD values retrieved from ATSR-2 data versus AOD retrieved from AERONET Sun photometer data is presented in Figure 5. The data are for 2 wavelengths, 0.555 μm and 0.659 μm and for different stations. In most of the cases the DV algorithm underestimates the AOD which is ascribed to the high absorbance of the aerosol present in the North-Western part of the area where most of the Sun photometers were located. The mean bias of the AOD values at 0.659 μm is 0.1 ± 0.1. Most of the less favorable comparisons occurred during the days of the large transport events. To evaluate the cause of the increasing discrepancy with increasing aerosol load, the data was split into two parts, for low and high AOD. The separation between low and high was, (somewhat arbitrarily) set at the mean AOD value determined from the AERONET measurements, i.e., AOD(0.67 μm) = 0.36. The mean difference between AOD from ATSR-2 and from AERONET measurements in the lower AOD range is 0.05 ± 0.04 and for the AOD values higher than the mean value 0.2 ± 0.1. Linear regression shows that the slope for the lower AOD range is 1.14, while the slope for the higher AOD values is 1.43. Best correlation occurs for the cleaner days with low concentration of absorbing aerosols. The correlation decreases for the days with high AOD values which are related to large transport events, and can be due to the assumption made in the DV algorithm that the reflectance varies linearly with the AOD, which at larger AODs may no longer be the case.

[31] Figure 6 shows the comparison of the temporal variation of the AOD measured with the Sun photometer at Mongu during August and September and the AOD retrieved from ATSR-2 data. Empty circles show the temporal variation of the Ångström coefficients. The two peaks in the Sun photometer AOD correspond to the two large transport events occurring during September 2000. During these events, the retrieval algorithm underestimated the AOD. However, outside of these, the retrieved AOD was in good agreement with the Sun photometer measurements. Ångström coefficients were also in good agreement with results presented by *Eck et al.* [2003] except for the transport events in September, when these authors obtained higher Ångström coefficient values. This increase in the Ångström coefficient is probably due to the increase in the fine mode aerosol concentration and, thus, a decrease in the relative influence of the coarse mode aerosols rather than to a change in the aerosol type. AERONET provides Ångström coefficient values computed at 0.500–0.870 μm at Mongu of about 1.8 to 2.0 during most of the SAFARI 2000 period. They obtained two days with very low values of 1.31 and 0.68 for the 15th and 22nd August respectively. On the other hand, in September there are three periods with high Ångström coefficient values of up to 2.1 on the 1st-3rd, 14th-16th, and 29th. It should be noted that these values are derived from data measured only at Mongu while retrieved Ångström coefficient values are derived from satellite data that covers most of Zambia.

6.3. Comparison With MODIS and MISR

[32] The Moderate Resolution Imaging Spectroradiometer (MODIS) and the Multiangle Imaging Spectroradiometer (MISR) are the most commonly used instruments to measure aerosol properties from space and are often used as a reference for other sensors. MODIS is an earth-viewing sensor that provides measurements in 36 spectral bands, from 0.415 to 14.235 μm with a spatial resolution that varies from 250 m to 1000 m depending on the band. As ATSR-2 MODIS uses different algorithms to retrieve AOD over land and over water. Over land 0.470 and 0.660 μm channels are used [*Kaufman et al.*, 1997]. However, unlike ATSR-2, MODIS has only a nadir view and the land surface reflectance at these wavelengths is corrected for by relating them to the reflectance at 2.12 μm. Recently, the assumptions involved were revised in the most recent version v5.2

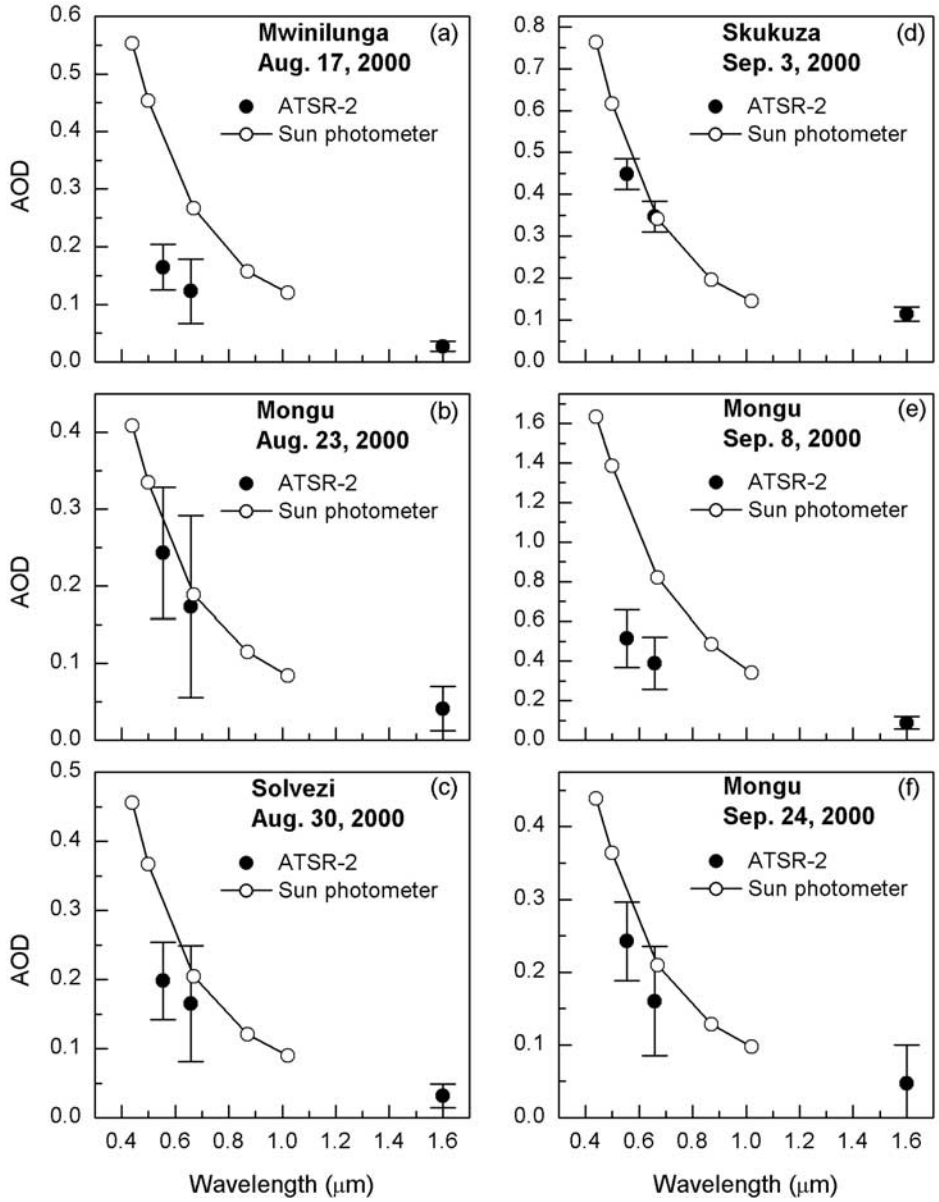

Figure 4. Comparison of the AOD measured by ground-based Sun photometers (empty circles) from the AERONET [*Holben et al.*, 1998] with retrieved AOD (solid circles) over land using the dual view algorithm at (a) Mwinilunga (24.43°E 11.74°S) on 17 August 2000, (b) Mongu (23.15°E 15.25°S) on 23 August 2000, (c) Solvezi (26.36°E 12.17°S) on 30 August 2000, (d) Skukuza (31.59°E 24.99°S) on 3 September 2000, (e) and (f) Mongu on 8 and 24 September 2000, respectively.

of the aerosol retrieval algorithm as described in detail by *Levy et al.* [2007a]. Also the set of aerosol model optical properties were replaced, based on AERONET measurements, and a new LUT was produced [*Levy et al.*, 2007b]. The resulting AOD data set, known as Collection 5 (or C005), significantly changed the global mean AOD from 0.28 in C004 to 0.21 in C005. This shows the significant influence of the underlying assumptions in the retrieval process. The C005 AOD meets expected accuracy levels of $\pm 0.05 \pm 0.15 \times$ AOD.

[33] Obviously C005 replaces C004 which should no longer be used. However, at the time when the current ATSR-2 study presented here was conducted, C005 was not available and therefore we compare with published MODIS results while keeping in mind that these may have changed. Similar to ATSR-2, MODIS C004 AOD values appear considerably underestimated when compared with several AERONET Sun photometers (Kaoma, Skukuza and Mongu) and the NASA Ames Airborne Tracking 14-channel Sun Photometer (AATS-14) measurements [*Schmid et al.*, 2003]. The results are better for Skukuza (in South Africa) than for Mongu (in Zambia) [*Schmid et al.*, 2003], likely because Mongu is closer to the fires and experiences different aerosol types than Skukuza which is further away and probably gets less absorbing aerosols. *Eck et al.* [2003] also found different aerosol properties in both stations.

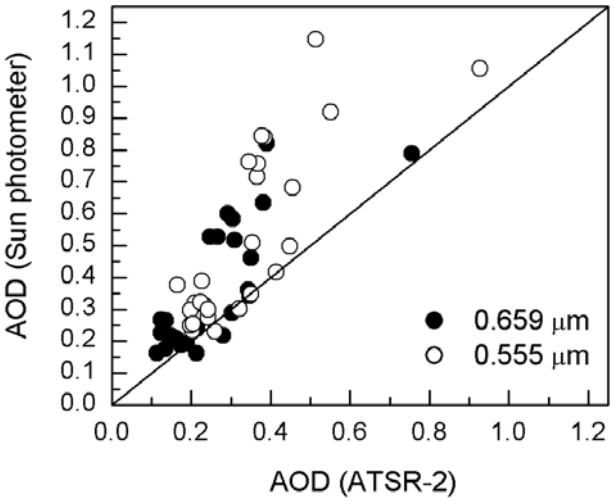

Figure 5. Scatterplot of the AOD from ATSR-2 and the Sun photometer at 0.555 μm (empty circles) and at 0.659 μm (solid circles) during August and September 2000. The straight line is where both results agree.

[34] MISR has nine discrete viewing angles to observe the Earth from nadir up to 70.5° forward and backward. Like ATSR-2, MISR takes advantage of differing angular reflectance signatures of the surface and the atmosphere to accomplish retrieval of AOD over land surface [*Diner et al.*, 2005]. Diner et al describe the MISR algorithm refinement that was implemented in 2003 and has its heritage in ATSR-2 work which is based on *Flowerdew and Haigh* [1995] and was first applied by *Veefkind et al.* [1998] for the retrieval of aerosol properties over land. The MISR algorithm also uses a set of LUTs that consider the most probable aerosols to be found in nature [*Martonchik et al.*, 1998, 2002]. The MISR LUT contains 24 aerosol components and allows for up to three lognormal modes [*Diner et al.*, 2005], whereas the ATSR-2 LUT used in this work allows for two lognormal components. A global comparison of AOD derived from MISR and AERONET ground based Sun photometer measurements was done by *Kahn et al.* [2005]. They found that about 2/3 of the MISR retrieved AOD values are within 0.05 of the AERONET AOD measurements and about 1/3 within 0.03. During the burning season in the SAFARI-2000 area the MISR AOD values in the midvisible part of the spectrum are skewed low due to the more absorbing aerosols that are found in the area [*Kahn et al.*, 2005].

[35] A recent comparison of AATSR (Advanced Along Track Scanning Radiometer, the successor of ATSR-2 with similar characteristics) over a moderately polluted area in Central Europe shows that the retrieval results of this instrument are similar to MODIS and MISR [*Kokhanovsky et al.*, 2007]. From an operational point of view, the differences are in the number of overpasses (MODIS twice daily, ATSR-2 every 3rd day ad MISR once a week), An advantage of ATSR is the long time series that started in 1995 with ATSR-1 on ERS-1, ATSR-2 on ERS2 and AATSR on ENVISAT, which will be continued with SLTS on Sentinel 3.

7. Discussion and Conclusions

[36] In this paper the feasibility to retrieve AOD and Ångström coefficients for absorbing aerosols from ATSR-2 data has been explored. Initially a different approach, which did not give the expected results, was followed. The idea was to detect and distinguish between highly absorbing aerosols from fresh smoke and less absorbing aged smoke. To this end, two different types of measurements during the SAFARI-2000 campaign were used to create two sets of LUTs. The first set of LUTs was created based on the physical and optical measurements done by *Haywood et al.* [2003] on the Met Office C-130 aircraft in Namibia. The second set was based on optical measurements from ground-based Sun photometers from *Dubovik et al.* [2002] and *Eck et al.* [2003].

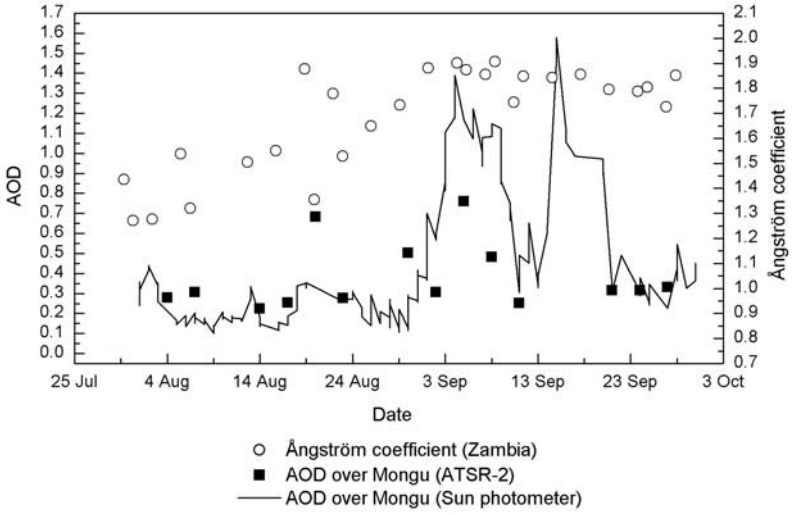

Figure 6. Temporal variation of the AOD over Mongu. The line represents the Sun photometer measurements. Solid squares show the retrieved AOD from ATSR-2 data. The empty circles are the Ångström coefficient values.

[37] Results from AOD retrievals with both sets of LUTs were compared with ground-based Sun photometer measurements from the AERONET database [*Holben et al.*, 1998] for September 2000 in order to determine which of them best represents the aerosol properties over the SAFARI-2000 area. It was found that none of them were able to accurately describe the high AOD values measured by the ground-based Sun photometers during two large transport events occurring in this month. Outside of these two periods the comparisons were reasonably good. In addition, the algorithm on no occasion found the highly absorbing aerosol type as the most probable. Therefore a less absorbing aerosol type was implemented in the algorithm that reproduced the optical properties of the aerosol present over the Southern areas of the experiment.

[38] When an absorbing aerosol layer is present in the atmosphere it absorbs both the incoming and the reflected solar radiation, thus inhibiting light to travel back to space. In that situation the amount of information about the lower part of atmosphere that reaches the satellite sensor is reduced. The highly absorbing capacity of the biomass burning aerosols is conjectured to be responsible for the lower accuracy of the AOD retrieval from the ATSR-2 data in the presence of high concentration of BB aerosols. As discussed in the previous section, dedicated aerosol instruments such as MODIS and MISR have similar problems with the retrieval of the AOD in the presence of highly absorbing biomass burning aerosol during the SAFARI-2000 campaign.

[39] Composite maps of the mean AOD, Ångström coefficients and relative contribution of two different absorbing aerosol types over the SAFARI-2000 dry season field campaign have been presented.

[40] During August 2000, AOD values of about 0.7–0.8 at 0.555 μm and Ångström coefficients of 1.7–2.1 were observed over the North-Western part of the SAFARI-2000 area. Over this area many fires occurred due to the presence of the tropical rain forest and savanna vegetation [http://earthobservatory.nasa.gov; *Diner et al.*, 2001]. In this region highly absorbing aerosols were detected. South of 10–15°S less absorbing aerosols were found with AOD values of up to 0.3 at 0.555 μm and Ångström coefficients of about 1.2. Over the Namibian and Kalahari deserts AOD of up to 0.75 at 0.555 μm was observed.

[41] In September the highly absorbing aerosols dominated over a larger area than in August, due to a change in the meteorological situation that caused advection of BB aerosol to the South.

[42] Comparisons with Sun photometer data from the AERONET database [*Holben et al.*, 1998] show that properties of the less-absorbing aerosol type can be retrieved with reasonable accuracy. The properties of the BB from the fires produced in the rain forest and savanna regions were not accurately retrieved due to their high absorption. However, an increase with retrieved AOD values was observed and in general the trend in the temporal evolution of the AOD was well reproduced.

[43] **Acknowledgments.** The work done in this paper was carried out while the authors were working at TNO Defense and Security, Oude Waalsdorperweg 63, P.O. Box 96864, 2509 JG, The Hague, The Netherlands and as part of the pHD thesis work of Christina Robles-Gonzalez. The work described in this paper was supported by SRON EO-037 and TNO internal funding. The ATSR-2 data was kindly provided by the European Space Agency (ESA-ESRIN). The authors thank B. Holben for the AERONET sun/sky radiometer data, P. Stammes for making his radiative transfer model available for this study, R. Koelemeijer for kindly providing his semi-automatic cloud detection algorithm, and P. Formenti for her help and for the fruitful discussions.

References

De Rooij, W. A., and C. C. A. H. van der Stap (1984), Expansion of Mie scattering in generalized spherical functions, *Astron. Astrophys.*, *131*, 237–248.

Diner, D. J., et al. (2001), MISR aerosol optical depth retrievals over southern Africa during the SAFARI-2000 dry season campaign, *Geophys. Res. Lett.*, *28*(16), 3127, doi:10.1029/2001GL013188.

Dubovik, O., B. N. Holben, T. F. Eck, A. Smirnov, Y. J. Kaufman, M. D. King, D. Tanre, and I. Slutsker (2002), Variability of absorption and optical properties of key aerosol types observed in worldwide locations, *J. Atm. Sci.*, *59*, 590–608.

Durkee, P. A., D. R. Jensen, E. E. Hindman, and T. H. VonderHaar (1986), The relationship between marine aerosols and satellite detected radiance, *J. Geophys. Res.*, *91*, 4063–4072.

Eck, T. F., et al. (2003), Variability of biomass burning aerosol optical characteristics in southern Africa during the SAFARI-2000 dry season campaign and a comparison of single scattering albedo estimates from radiometric measurements, *J. Geophys. Res.*, *108*(D13), 8477, doi:10.1029/2002JD002321.

Flowerdew, R. J., and J. D. Haigh (1995), An approximation to improve accuracy in the derivation of surface reflectances from multi-look satellite radiometers, *Geophys. Res. Lett.*, *23*, 1693–1696.

De Haan, J. F., P. B. Bosma, and J. W. Hovenier (1987), The adding method for multiple scattering calculations of polarized light, *Astron. Astrophys.*, *183*, 371–391.

Diner, D. J., J. V. Martonchik, R. A. Kahn, B. Pinty, N. Gobron, D. L. Nelson, and B. N. Holben (2005), Using angular and spectral shape similarity constraints to improve MISR aerosol and surface retrievals over land, *Remote Sens. Environ.*, *94*, 155–171.

Haywood, J. M., S. R. Osborne, P. N. Francis, A. Keil, P. Formenti, M. O. Andreae, and P. H. Kaye (2003), The mean physical and optical properties of regional haze dominated by biomass burning aerosol measured from the C-130 aircraft during SAFARI 2000, *J. Geophys. Res.*, *108*(D13), 8473, doi:10.1029/2002JD002226.

Holben, B. N., et al. (1998), AERONET- A federated instrument network and data archive for aerosol characterisation, *Remote Sens. Environ.*, *66*, 1–16.

Iacobellis, S. F., R. Frouin, and R. C. J. Somerville (1999), Direct climate forcing by biomass-burning aerosols: Impact of correlations between controlling variables, *J. Geophys. Res.*, *104*(D10), 12,031–12,045.

IPCC (2001), Climate Change 2001: The Scientific Basis, in *Contribution of Working Group I to the Third Assessment Report of the Intergovernmental Panel on Climate Change*, edited by J. T. Houghton, Y. Ding, D. J. Griggs, M. Noguer, P. J. van der Linden, X. Dai, K. Maskell, and C. A. Johnson, pp. 881, Cambridge University Press, Cambridge, United Kingdom and New York, NY, USA.

IPCC (2007), Climate Change 2007: The Physical Science Basis, in *Contribution of Working Group I to the Fourth Assessment Report of the Intergovernmental Panel on Climate Change*, edited by S. Solomon, D. Qin, M. Manning, Z. Chen, M. Marquis, K. B. Averyt, M. Tignor and H. L. Miller, pp. 996, Cambridge University Press, Cambridge, United Kingdom and New York, NY, USA.

Kahn, R. A., B. J. Gaitley, J. V. Martonchik, D. J. Diner, K. A. Crean, and B. Holben (2005), Multiangle Imaging Spectroradiometer (MISR) global aerosol optical depth validation based on 2 years of coincident Aerosol Robotic Network (AERONET) observations, *J. Geophys. Res.*, *110*, D10S04, doi:10.1029/2004JD004706.

Kaufman, Y. J., D. Tanre, L. Remer, E. F. Vermote, A. Chu, and B. N. Holben (1997), Operational remote sensing of tropospheric aerosol over the land from EOS-MODIS, *J. Geophys. Res.*, *102*(14), 17,051–17,068.

Koelemeijer, R. B. A., P. Stammes, J. W. Hovenier, and J. D. De Haan (2001), A fast method for retrieval of cloud parameters using oxygen A-band measurements from the Global Ozone Monitoring Instrument, *J. Geophys. Res.*, *106*, 3475–3490.

Kokhanovsky, A. A., R. L. Curier, G. de Leeuw, W. M. F. Grey, K.-H. Lee, Y. Bennouna, R. Schoemaker, and P. R. J. North (2007), The inter-comparison of AATSR dual view aerosol optical thickness retrievals with results from various algorithms and instruments, submitted to Int. J. Remote Sensing.

Levy, R. C., L. A. Remer, S. Mattoo, E. Vermote, and Y. J. Kaufman (2007a), The second generation operational algorithm for retrieving aerosol properties over land from MODIS spectral reflectance, *J. Geophys. Res.*, *112*, D13211, doi:10.1029/2006JD007811.

Levy, R. C., et al. (2007b), Global aerosol optical properties and application to MODIS aerosol retrieval over land, *J. Geophys. Res.*, *112*, D13210, doi:10.1029/2006JD007815.

Martonchik, J. V., D. J. Diner, R. A. Kahn, T. P. Ackerman, M. M. Verstraete, B. Pinty, and H. R. Gordon (1998), Techniques for the retrieval of aerosol properties over land and ocean using multiangle imaging, *IEEE Trans. Geosci. Remote Sens.*, *36*, 1212–1227.

Martonchik, J. V., D. J. Diner, K. A. Crean, and M. A. Bull (2002), Regional aerosol retrieval results from MISR, *IEEE Trans. Geosci. Remote Sens.*, *40*, 1520–1531.

Myhre, G., T. K. Berntsen, J. M. Haywwod, J. K. Sundet, B. N. Holben, M. Johnsrud, and F. Stordal (2003), Modelling the solar radiative impact of aerosols from biomass burning during SAFARI-2000, *J. Geophys. Res.*, *108*(D13), 8501, doi:10.1029/2002JD002313.

North, P. R. J. (2002), Estimation of aerosol opacity and land surface bidirectional reflectance from ATSR-2 dual-angle imagery: Operational method and validation, *J. Geophys. Res.*, *107*(D12), 4149, doi:10.1029/2000JD000207.

Robles-Gonzalez, C. (2003), Retrieval of Aerosol Properties using ATSR-2 Observations and their Interpretation, PhD Thesis, University of Utrecht, Utrecht, The Netherlands.

Robles González, C., J. P. Veefkind, and G. de Leeuw (2000), Aerosol optical depth over Europe in August 1997 derived from ATSR-2 data, *Geophys. Res. Lett.*, *27*(7), 955–958.

Robles-Gonzalez, C., G. de Leeuw, R. Decae, J. Kusmierczyk-Michulec, and P. Stammes (2006), Aerosol properties over the Indian Ocean Experiment (INDOEX) campaign area retrieved from ATSR-2, *J. Geophys. Res.*, *111*, D15205, doi:10.1029/2005JD006184.

Schmid, B., et al. (2003), Coordinated airborne, spaceborne, and ground-based measurements of massive, thick aerosol layers during the dry season in southern Africa, *J. Geophys. Res.*, *108*(D13), 8496, doi:10.1029/2002JD002297.

Stammes, P. (2001), Spectral radiance modelling in the UV-Visible range, in *IRS 2000: Current problems in Atmospheric Radiation*, edited by W. L. Smith and Y. M. Timofeyev, pp. 385–388, A. Deepak Publ., Hampton, VA.

Stricker, N. C. M., A. Hahne, D. L. Smith, J. Delderfield, M. B. Oliver, and T. Edwards (1995), ATSR-2: The evolution in its design from ERS-1 to ERS-2, ESA Bulletin-European Space Agency, No.83, 32–37.

Swap, R. J., et al. (2002), The Southern African Regional Science Initiative (SAFARI 2000): Overview of the dry season field campaign, *South Afr. J. Sci.*, *98*, 125.

Veefkind, J. P., G. de Leeuw, and P. A. Durkee (1998), Retrieval of Aerosol Optical Depth over Land using two angle view satellite radiometry during TARFOX, *Geophys. Res. Lett.*, *25*, 3135–3138.

Wang, M., and H. R. Gordon (1994), Radiance reflected from the ocean atmosphere system: Synthesis from individual components of aerosol size distribution, *Appl. Opt.*, *33*, 7088–7095.

Ward, D. E., R. A. Susott, J. B. Kaufman, R. E. Babbitt, D. L. Cummings, B. Dias, B. N. Holben, Y. J. Kaufman, R. A. Rasmussen, and A. W. Setzer (1992), Smoke and fire characteristics for Cerrado and deforestation burns in Brazil: Base-B experiment, *J. Geophys. Res.*, *97*, 14,601–14,619.

Ward, D. E., W. M. Hao, R. A. Susott, R. E. Babbitt, R. W. Shea, J. B. Kaufman, and C. O. Justice (1996), Effect of fuel composition on combustion efficiency and emission factors for African savanna ecosystems, *J. Geophys. Res.*, *101*, 23,569–23,576.

G. de Leeuw, Finnish Meteorological Institute, R&D, Climate Change Unit, Modelling and Observation of Atmosphere, Helsinki, Finland.

C. Robles-Gonzalez, National Spanish Institute for Aerospace Technology (INTA), Ajalvir road km 4, 28850 Torrejon de Ardoz, Madrid, Spain. (roblesgc@inta.es)